

# QUANTIZED MASSIVE SCALAR FIELDS IN THE SPACETIME OF A CHARGED DILATONIC BLACK HOLE. ENERGY CONDITIONS

JERZY MATYJASEK

Institute of Physics, Maria Curie-Skłodowska University  
pl. Marii Curie-Skłodowskiej 1, 20-031 Lublin, Poland  
e-mail: [matyjase@tytan.umcs.lublin.pl](mailto:matyjase@tytan.umcs.lublin.pl)  
[jurek@kft.umcs.lublin.pl](mailto:jurek@kft.umcs.lublin.pl)

*(Received February 24, 2003)*

Employing the approximate effective action constructed from the coincidence limit of the Hadamard–Minakshisundaram–DeWitt (HaMiDeW) coefficient  $a_3$ , the renormalized stress-energy tensor of the quantized massive scalar field in the spacetime of a static and electrically charged dilatonic black hole is calculated. Special attention is paid to the minimally and conformally coupled fields propagating in geometries with  $a = 1$ , and to the power expansion of the general stress-energy tensor for small values of charge. A compact expression for the trace of the stress-energy tensor is presented. Finally, various pointwise energy conditions are considered.

PACS numbers: 04.62.+v, 04.70.Dy

## 1. Introduction

According to our present understanding the physical content of quantum field theory formulated in a spacetime describing black hole is contained in the renormalized stress-energy tensor,  $\langle T^{ab} \rangle$ , evaluated in a physically motivated state [1]. And although interesting in its own, the stress-energy tensor plays a crucial role in various applications, most important of which is the problem of back reaction on the metric. Indeed, treating the stress-energy tensor as a source term of the semi-classical Einstein fields equations, one may, in principle, investigate the evolution of the system unless the quantum gravity effects become dominant. Unfortunately, this program is hard to execute as the semi-classical field equations comprise rather complicated set of nonlinear partial differential equations, and, moreover, it requires knowledge of functional dependence of  $\langle T^{ab} \rangle$  on a wide class of metrics. It is natural,

therefore, that in order to answer — at least partially — this question, one should refer either to approximations or to numerical methods.

It seems that for the massive fields in a large mass limit, *i.e.*, when the Compton length,  $l_C$ , is much smaller than the characteristic radius of curvature,  $\mathbb{L}$ , (where the latter means any characteristic length scale of the spacetime), the approximation based on the asymptotic Schwinger–DeWitt expansion is of the required generality [2–4]. Since the nonlocal contribution to the effective action could be neglected it is expected that the method yields reasonable results provided the gravitational field is weak and its temporal changes remain small. Despite of the above restrictions there is still a wide class of geometries in which the approximation could be successfully applied.

For a neutral massive scalar field with an arbitrary curvature coupling satisfying

$$(\square - \xi R - m^2) \phi = 0, \quad (1.1)$$

where  $\xi$  is the coupling constant and  $m$  is the mass of the field, the approximate renormalized effective action,  $W_R$ , may be expanded in powers of  $m^{-2}$  [5–7]. The  $n$ -th term of the expansion involves coincidence limit of the Hadamard–Minakshisundaram–DeWitt (HaMiDeW [8]) coefficient  $[a_n]$  constructed solely from the curvature tensor, its covariant derivatives up to  $2n - 2$  order and appropriate contractions [3, 9–15]. As the complexity of the ‘HaMiDeW’ coefficients rapidly grows with increasing  $n$  their practical use is limited to  $n = 3$ , perhaps  $n = 4$ . Moreover, it should be emphasized that the Schwinger–DeWitt expansion is asymptotic and adding more terms does not necessarily improve the approximation. Here we shall confine ourselves to the simplest yet computationally involved case  $n = 3$ , in which the approximate effective action could be written as

$$W_R = \frac{1}{32\pi^2} \int d^4x \sqrt{g} \frac{1}{m^2} [a_3]. \quad (1.2)$$

Having at one’s disposal the approximation of the renormalized effective action, the stress-energy tensor could be evaluated by means of the standard formula

$$\frac{2}{\sqrt{g}} \frac{\delta}{\delta g_{ab}} W_R = \langle T^{ab} \rangle. \quad (1.3)$$

Since the coefficient  $[a_3]$  is rather complicated so is the stress-energy tensor and the question arose of a practical applicability of the thus obtained results. Fortunately it could be used in a number of physically interesting and important cases. The method has been employed by Frolov and Zel’nikov in a series of papers [5–7] devoted to construction of  $\langle T^{ab} \rangle$  of the massive

scalar, spinor and vector fields in vacuum type-D spacetimes and generalized recently to arbitrary geometries in [16,17]. General formulas describing  $\langle T^{ab} \rangle$  consist of over 100 local terms.

The effective action technique that we employ in this paper requires the metric of the spacetime to be positively defined. Hence, to obtain the physical stress-energy tensor one has to analytically continue at the final stage of calculations its Euclidean counterpart.

An alternative approach based on the WKB approximation of the solutions to the radial equation and summation of the mode functions has been developed by Anderson, Hiscock, and Samuel [18] (see also [19]), who, among other things, succeeded in construction of the general form of the stress-energy tensor of the scalar field in a large mass limit in a static and spherically-symmetric geometry. Both approaches give, as expected, identical results and the detailed numerical analyses carried out by these authors show that for  $mM \gtrsim 2$  ( $M$  is the black hole mass) the accuracy of the Schwinger–DeWitt approximation in the Reissner–Nordström geometry is quite good (1% or better) [20]. The Schwinger–DeWitt method has been employed in various contexts in [16–18, 20–26]. (The case of the massive spinor field is currently actively investigated [27].)

In this article we shall study the stress-energy tensor of the quantized massive scalar field with an arbitrary curvature coupling in a background of the static spherically-symmetric charged dilatonic black holes which are the solutions of the coupled system of the Einstein–Maxwell-dilaton equations. Such solutions are characterized by mass  $M$  and by electric  $Q$  and dilatonic  $a$  charges [28,29]. For some particular choices of the parameter  $a$  the solutions of the system are especially interesting. Indeed,  $a = 0$  corresponds to the Reissner–Nordström solution,  $a = 1$  to the solution obtained from the low energy limit of the string effective action, whereas  $a = \sqrt{3}$  to the four dimensional effective model reduced from the Kaluza–Klein theory in five dimensions. Despite of this we do not relate our considerations with the specific model, rather, we shall concentrate on the influence of the geometry on the approximate renormalized stress-energy tensor. Although all informations regarding quantized fields in the curved background are encoded in the components of the stress-energy tensor themselves, to gain a better understanding of the nature of quantized fields we shall examine pointwise energy conditions and show that in the spacetime of the dilatonic black hole they are violated in an interesting way.

Various properties of charged dilatonic black holes have been examined in a numerous papers. On the other hand however, quantum effects in 4D dilatonic black hole are — to the best of my knowledge — practically unexplored. This does not mean that this group of problems is uninteresting: belonging to the realm of the low-energy approximation to string theory

or the Kaluza–Klein theory, the dilatonic black holes would interact with various quantized fields. The main obstacle preventing construction of the renormalized stress-energy tensor is the computational complexity of the problem.

The evaporation process of the massless scalar field noninteracting with a dilaton field has been analyzed in [30, 31] whereas the field fluctuation,  $\langle \phi^2 \rangle$ , of the minimally coupled massless scalar field in the vicinity of the event horizon of the dilatonic black hole has been studied by Shiraishi [32]. Specifically, it was shown that the emission rate of the Hawking radiation blows up near the extremality limit for  $a > 1$ . On the other hand it is finite for  $a = 1$  and zero for  $a < 1$ . The field fluctuation diverges for  $a > 0$  for the extremal configuration.

Some aspects of the massless quantum fields in the spacetime of 2D dilatonic black holes have been discussed in Ref. [33]. Specifically, it was shown that in order for the stress-energy tensor to be regular in the geometry of the extreme string metric it is necessary to assign a definite nonzero temperature.

## 2. The geometry

Let us consider the action:

$$S = \int d^4x \sqrt{-g} \left[ R - 2 (\nabla \phi)^2 - e^{-2a\phi} F^2 \right], \quad (2.1)$$

where  $\phi$  is the massless dilatonic field,  $F$  is the strength of the Maxwell field ( $F_{ab} = 2\nabla_{[a}A_{b]}$ ) and  $a$  is the coupling constant. We recall that the choice  $a = 1$  corresponds to the low energy limit of the string effective action,  $a = \sqrt{3}$  to the four dimensional effective model reduced from the Kaluza–Klein theory in five dimensions, and the Einstein–Maxwell system is obtained with  $a = 0$ . Modifications of the action (2.1) are considered, for example, in [34, 35].

For each value of the parameter  $a$  there exists a black hole solution depending on the electric charge and the mass [28, 29]. Indeed, functionally differentiating  $S$  with respect to the metric tensor, dilaton field, and Maxwell field one obtains the system of the Einstein–Maxwell-dilaton equations of motion that could be solved exactly. Static and spherically-symmetric solution has been found by Gibbons [28], and by Garfinkle, Horowitz and Strominger [29]:

$$ds^2 = A(r) dt^2 + \frac{dr^2}{A(r)} + B^2(r) d\Omega^2, \quad (2.2)$$

where

$$A(r) = \left(1 - \frac{r_+}{r}\right) \left(1 - \frac{r_-}{r}\right)^{\frac{1-a^2}{1+a^2}} \quad (2.3)$$

and

$$B^2 = r^2 \left(1 - \frac{r_-}{r}\right)^{\frac{2a^2}{1+a^2}}. \quad (2.4)$$

The integration constants  $r_+$  and  $r_-$  are related to the mass and charge of the dilatonic black hole according to

$$2M = r_+ + \left(\frac{1-a^2}{1+a^2}\right) r_- \quad (2.5)$$

and

$$Q^2 = \frac{r_+ r_-}{1+a^2}. \quad (2.6)$$

The dilaton field is given by

$$e^{2a\phi} = \left(1 - \frac{r_-}{r}\right)^{\frac{2a^2}{1+a^2}}, \quad (2.7)$$

whereas the electric field is simply  $F = \frac{Q}{r^2} dt \wedge dr$ . Inspection of the line element shows that the event horizon is located at  $r_+$ ; at  $r = r_-$  one has a coordinate singularity that could be ignored so long one considers region  $r \geq r_+ > r_-$ . The choice  $a = 0$  leads to the Reissner–Nordström solution. At  $|Q|/M = (1+a^2)^{1/2}$ , a case usually addressed to as an extremal black hole, the event horizon and  $r_-$  coincide and in this limit the surface  $r = r_+ = r_-$  is zero except  $a = 0$ . Although more realistic models require massive  $\phi$  field, the dilatonic solutions (2.2)–(2.4) are of principal interest as they provide useful models for studies of the consequences of modifications of the geometries of the classical black holes. Finally, observe that the Kretschmann scalar  $K$  computed at the event horizon near the extremality limit behaves as

$$K \sim (r_+ - r_-)^{-\frac{4a^2}{1+a^2}}. \quad (2.8)$$

### 3. The renormalized stress-energy tensor

#### 3.1. Approximate effective action

In the framework of the Schwinger–DeWitt approximation the first order effective action of the massive scalar field is constructed from the coincidence limit of the coefficient  $a_3(x, x')$ . Inserting  $[a_3]$  as given in Appendix into

(1.2), integrating by parts and finally making use of the elementary properties of the Riemann tensor, after necessary simplifications one has [12–14]:

$$\begin{aligned}
 W_{\text{ren}}^{(1)} &= \frac{1}{192\pi^2 m^2} \int d^4x \sqrt{g} \left[ \frac{1}{2} \left( \eta^2 - \frac{\eta}{15} - \frac{1}{315} \right) R \square R + \frac{1}{140} R_{pq} \square R^{pq} \right. \\
 &\quad - \eta^3 R^3 + \frac{1}{30} \eta R R_{pq} R^{pq} - \frac{1}{30} \eta R R_{pqab} R^{pqab} - \frac{8}{945} R_q^p R_a^q R_p^a \\
 &\quad + \frac{2}{315} R^{pq} R_{ab} R_p^a R_q^b + \frac{1}{1260} R_{pq} R_{cab} R^{qcab} + \frac{17}{7560} R_{ab}{}^{pq} R_{pq}{}^{cd} R_{cd}{}^{ab} \\
 &\quad \left. - \frac{1}{270} R_p^a R_q^b R_c^p R_d^q R_{ab}{}^{cd} \right] \\
 &= \frac{1}{192\pi^2 m^2} \sum_{i=1}^{10} \alpha_i W_{(i)}, \tag{3.1}
 \end{aligned}$$

where  $\eta = \xi - 1/6$  and  $\alpha_i$  are equal to the numerical coefficients that stand in front of the geometrical terms in the right-hand side of the equation (3.1).

Differentiating functionally  $W_{\text{ren}}^{(1)}$  with respect to a metric tensor one obtains rather complicated expression which schematically may be written as

$$\begin{aligned}
 \langle T^{ab} \rangle &= \sum_{i=1}^{10} \alpha_i \tilde{T}^{(i)ab} = \frac{1}{96\pi^2 m^2 \sqrt{g}} \sum_{i=1}^{10} \alpha_i \frac{\delta W_{(i)}}{\delta g_{ab}} \\
 &= T^{(0)ab} + \eta T^{(1)ab} + \eta^2 T^{(2)ab} + \eta^3 T^{(3)ab}. \tag{3.2}
 \end{aligned}$$

Each  $\tilde{T}^{(i)ab}$  is constructed solely from the curvature tensor, its covariant derivatives and appropriate contractions. Because of the complexity of the resulting stress-energy tensor it will be not presented here and for its full form as well as the technical details the reader is referred to [16, 17]. It should be emphasized that because of the form of the dilatonic metric, the method presented in Refs [16] and [17] is the only one capable of the direct evaluation of the stress-energy tensor in the large mass limit. Moreover, this results may be easily extended to fields of other spins as the appropriate tensors differ by the numerical coefficients  $\alpha_i$  only.

The coincidence limit of  $a_4(x, x')$  is known: it has been calculated by Avramidi [12–14] and by Amsterdamski, Berkin and O'Connor [15]. Consequently the method could be extended, in principle, to include  $m^{-4}$  terms. Unfortunately, since the effective action constructed from  $[a_4]$  is extremely complicated, so is its functional derivative and the practical use of the thus obtained result may be a real challenge. However,  $[a_4]$  still could be employed in the analyses of the field fluctuation. The general structure of  $[a_4]$

indicates that the second-order stress-energy tensor divides naturally into five terms  $\sum_{i=0}^4 \eta^i T^{(i)ab}$ .

In order to simplify our discussion let us define  $q = |Q|/M$ ,  $x_{\pm} = r_{\pm}/M$  and  $x = r/M$ . The Schwinger–DeWitt technique may be used when the characteristic radius of curvature is much greater than the Compton length. Simple considerations indicate that for  $r \gg r_+$  it could be used for arbitrary value of  $a$ . Assuming that  $\mathbb{L}$  is related to the Kretschmann scalar as

$$R_{abcd}R^{abcd} \sim \mathbb{L}^{-4}, \quad (3.3)$$

the condition of applicability of the approximation near the event horizon could be written as

$$\frac{2c}{M^2 x_+^3} (x_+ - x_-)^{-\frac{2a^2}{1+a^2}} \ll m^2, \quad (3.4)$$

where  $c^2 = 2x_-^2 + [x_- - (1+a^2)x_+]^2$ . It is evident that for  $a > 0$  the Schwinger–DeWitt approximation is inapplicable for  $r_+$  close to  $r_-$ . For the extremal Reissner–Nordström black hole this condition becomes  $M^2 m^2 \gg 2\sqrt{2}$ .

The temperature of the dilatonic black hole obtained by means of standard methods is given by

$$T_H = \frac{1}{4\pi M x_+} \left( 1 - \frac{x_-}{x_+} \right)^{\frac{1-a^2}{1+a^2}} \quad (3.5)$$

and for given  $q$  it depends on the dilatonic coupling. Inspection of (3.5) shows that

$$\begin{aligned} T_H &< (8\pi M)^{-1} & (a < 1), \\ T_H &= (8\pi M)^{-1} & (a = 1), \\ T_H &> (8\pi M)^{-1} & (a > 1). \end{aligned}$$

The temperature of the extremal configuration is zero for  $a < 1$ , takes the same value as for a Schwarzschild black hole for  $a = 1$ , and diverges for  $a > 0$ . Moreover, it is easily seen that the condition  $T_H \ll m$  is violated for  $a > 1$  near the extremality limit.

### 3.2. General case

Solving the system (2.5) and (2.6) one easily obtains

$$x_+ = 1 + \sqrt{1 - (1 - a^2)q^2} \quad (3.6)$$

and

$$x_- = \frac{1+a^2}{1-a^2} \left( 1 - \sqrt{1 - (1-a^2)q^2} \right). \quad (3.7)$$

Before proceeding further let us observe that  $R = 0$  for  $a = 0$ , and, consequently,  $\delta W_{(1)}/\delta g_{ab}$  and  $\delta W_{(3)}/\delta g_{ab}$  is zero. The stress-energy tensor has therefore a simple form

$$\langle T_a^b \rangle^{a=0} = T_a^{(0)b} + \eta T_a^{(1)b}. \quad (3.8)$$

On the other hand, the curvature scalar vanishes at the event horizon for any  $a$  and is  $\mathcal{O}(q^4)$  for small  $q$  elsewhere. Moreover, since  $\partial_r R$  is the only nonzero component of  $\nabla_a R$  one concludes that  $T_a^{(3)b}(r_+) = 0$  and is negligible in the closest vicinity of  $r_+$ . It is because the only non-vanishing in this limit term is proportional to

$$\nabla_a R \nabla^b R - (\nabla R)^2 \delta_a^b. \quad (3.9)$$

A closer examination indicates that  $T_a^{(3)b}$  is  $\mathcal{O}(q^8)$ . Similarly, one expects that for small  $q$  the term  $T_a^{(2)b}$  is of order  $\mathcal{O}(q^4)$ . On the other hand, the contribution of the last two terms in the right-hand side of equation (3.2) could be made arbitrarily large by a suitable choice of the curvature coupling. It should be noted however that such values of  $\eta$  are clearly unphysical and should be rejected.

Restricting to the exterior region and calculating components of the Riemann tensor, its contractions and covariant derivatives to the required order, after some algebra, one arrives at the rather complicated result, that for obvious reasons will not be presented here. However, it could be schematically written in surprisingly simple form

$$\langle T_a^b \rangle = \frac{p}{(1+a^2)x^{15}} \left( 1 - \frac{x_-}{x} \right)^{-\frac{3(3a^2+1)}{1+a^2}} \sum_{ijk} d_{ijk}^a [\eta, a^2] x^i x_+^j x_-^k, \quad (3.10)$$

with  $0 \leq i \leq 7$ ,  $0 \leq j \leq 3$  and  $0 \leq k \leq 6$  subjected to the condition  $i + j + k = 9$ . Here

$$p = \frac{1}{192\pi^2 m^2 M^6} \quad (3.11)$$

and  $d_{ijk}^a$  for given  $a$  and  $\eta$  are numerical coefficients. Some extra work shows that the tensor (3.10) is covariantly conserved and is regular for regular geometries. Moreover, the difference  $\langle T_t^t \rangle - \langle T_r^r \rangle$  factors

$$\langle T_t^t \rangle - \langle T_r^r \rangle = \frac{p}{(1+a^2)x^{14}} \left( 1 - \frac{x_+}{x} \right) \left( 1 - \frac{x_-}{x} \right)^{-\frac{3(3a^2+1)}{1+a^2}} f(x), \quad (3.12)$$

where the regular function  $f \sim (x_+ - x_-)^2$  as  $x_- \rightarrow x_+$  and consequently within the domain of applicability of the Schwinger–DeWitt approximation the stress-energy tensor is regular in a freely falling frame.

It could be demonstrated that the trace of the stress-energy tensor of the quantized massive scalar field has a simple form

$$\langle T_a^a \rangle = \frac{1}{16\pi^2 m^2} \left\{ 3 \left( \xi - \frac{1}{6} \right) \square [a_2] - [a_3] \right\}. \quad (3.13)$$

This equation together with

$$\nabla_b T_a^b = 0 \quad (3.14)$$

may serve as an independent check of the calculations. On the other hand however, it suffices to calculate only one component of the stress-energy tensor, say  $\langle T_t^t \rangle$ , as the remaining ones could be obtained with the aid of (3.13) and (3.14).

For conformally coupled fields the trace is proportional to the coincidence limit of  $[a_3]$ . We remark here that for conformally invariant massless scalar field the anomalous trace is proportional to  $[a_2]$ ; it should be noted however, that (3.13) has been calculated for  $\langle T_a^b \rangle$  given by (3.2) whereas the trace of the conformally invariant massless fields is a general property of the regularized stress-energy tensor.

Since the practical use of the general result is limited, it is instructive to analyze the stress-energy tensor in some specific cases. In the latter we shall confine our analysis to  $0 \leq a \leq \sqrt{3}$  with the special emphasis put on the case  $a = 1$ . However, before proceeding to examination of some concrete choices of  $a$  let us analyze a general  $\langle T_a^b \rangle$  for small  $q$ .

### 3.3. Arbitrary $a$ , $q \ll 1$

Assuming  $q \ll 1$ , expanding  $\langle T_a^b \rangle$  into a power series, and finally collecting the terms with the like powers of  $q$  one has

$$\langle T_a^b \rangle = \langle T_a^b \rangle^{a=0} + \frac{a^2}{96\pi^2 m^2 x^{10} M^6} (q^2 t_a^{(1)b} + q^4 t_a^{(2)b} + q^6 t_a^{(3)b} + \dots), \quad (3.15)$$

where  $\langle T_b^b \rangle^{a=0}$  is evaluated for  $a = 0$  and coincides with the expression describing the stress-energy tensor in the geometry of the Reissner–Nordström black hole [16, 18]. The explicit expressions for the coefficients  $t_a^{(i)b}$  as well as the components of  $\langle T_b^b \rangle^{a=0}$  are listed in the appendix. A closer examination shows that for  $q \lesssim 0.7$  the expansion (3.15) reproduces the general result satisfactorily, and, moreover, for  $q \lesssim 1/3$  the results weakly depend on the coupling  $a$ . From (3.15) it is evident that for  $a = 0$  and  $q = 0$  the stress-energy tensor reduces to the expression derived by Frolov and Zel'nikov in the geometry of the Schwarzschild black hole [5, 36].

### 3.4. Dilatonic black hole $a = 1$

In this subsection we shall construct and investigate the stress-energy tensor of the massive scalar field resulting from (3.10) for the particular combinations of couplings. Consider  $a = 1$ . Since the second factor in  $A(r)$  vanishes, we expect considerable simplifications as the event horizon is now located at  $2M$  whereas the ‘inner’ one at  $q^2M$ . Indeed, defining  $y = r/r_+$ , equation (3.10) could be written in a simple form:

$$\langle T_a^b \rangle = \frac{p}{(2y - q^2)^6} \sum_{ij} b_{ija}^b [\eta] q^{2i} y^{-j-2} \quad (3.16)$$

with  $0 \leq i \leq 6$  and  $0 \leq j \leq 7$ , where  $b_{ija}^b$  are numerical coefficients. From (3.12) it could be shown that for any  $\eta$  the difference  $\langle T_t^t \rangle - \langle T_r^r \rangle$  factorizes as

$$\langle T_t^t \rangle - \langle T_r^r \rangle = \frac{1 - y}{y^9 (q^2 - 2y)^6} f(y), \quad (3.17)$$

where, for  $0 \leq q < \sqrt{2}$  the function  $f(y)$  is regular at the event horizon. Equation (3.16) could be contrasted to the analogous expression evaluated in the Reissner–Nordström geometry ( $a = 0$ ) :

$$\langle T_a^b \rangle = \frac{p}{y^6} \sum_{ij} c_{ija}^b [\eta] q^{2i} y^{-j-2}, \quad (3.18)$$

where  $0 \leq i \leq 3$ ,  $0 \leq j \leq 4$ , and  $c_{ija}^b$  is another set of numerical coefficients.

To perform quantitative analysis however, we have to refer to exact formulas. For  $\eta = 0$  it suffices to compute only  $T_a^{(0)b}$  as the other terms do not contribute to the final result. Moreover, it suffices to know only one component of the stress-energy tensor, say  $\langle T_t^t \rangle$ , as the remaining ones could be easily obtained solving equations (3.13) and (3.14) and putting the integration constant to zero. The conservation equation for the line element (2.2) has the following form

$$\frac{d}{dr} \langle T_r^r \rangle - w_1(r) \langle T_a^a \rangle + w_2(r) \langle T_r^r \rangle + w_3(r) \langle T_t^t \rangle = 0, \quad (3.19)$$

where

$$w_1(r) = \frac{r - r_- + a^2 r}{(r - r_-)(1 + a^2)}, \quad (3.20)$$

$$w_2(r) = \frac{6a^2 r^2 - 5r_+ r - 5r_- r + 4r_+ r_- + 6r^2 - a^2 r_- r - 5a^2 r_+ r}{r(1 + a^2)(r - r_+)(r - r_-)}, \quad (3.21)$$

and

$$w_3(r) = \frac{6r_+r_- - 5r_+r - 5r_-r + 4a^2r^2 + a^2r_-r - 5a^2r_+r + 4r^2}{r(1+a^2)(r-r_+)(r-r_-)}. \quad (3.22)$$

After some algebra one has

$$\langle T_t^t \rangle = \frac{p}{(2y-q^6)} \sum_{i=0}^6 f_i q^{2i}, \quad (3.23)$$

where

$$\begin{aligned} f_0(y) &= \frac{313}{210y^3} - \frac{19}{14y^2}, & f_1(y) &= -\frac{61}{30y^4} = \frac{31}{70y^3} = \frac{9}{7y^2}, \\ f_2(y) &= \frac{143}{840y^5} + \frac{7313}{2520y^4} - \frac{577}{210y^3} - \frac{1}{28y^2}, \\ f_3(y) &= \frac{1381}{1120y^6} - \frac{6607}{1680y^5} + \frac{1813}{720y^4} + \frac{1}{28y^3}, \\ f_4(y) &= -\frac{9277}{10080y^7} + \frac{43837}{20160y^6} - \frac{1007}{840y^5} - \frac{139}{10080y^4}, \\ f_5(y) &= \frac{1817}{6720y^8} - \frac{479}{840y^7} + \frac{559}{1920y^6} + \frac{7}{2880y^5}, \\ f_6(y) &= -\frac{1783}{60480y^9} + \frac{473}{8064y^8} - \frac{11}{384y^7} - \frac{1}{6912y^6}. \end{aligned} \quad (3.24)$$

To avoid unnecessary proliferation of long formulas we displayed only one component of the stress-energy tensor.

Despite its similarity with the Schwarzschild line element, the non-extremal  $a = 1$  dilatonic black holes have much in common with the Reissner–Nordström solution. We shall, therefore, address the question of how the differences between the geometry of the Reissner–Nordström black hole on the one hand and the dilatonic black hole on the other are reflected in the overall behavior of our approximate stress-energy tensors. First, from the form of the stress-energy tensor it could be easily inferred that  $\langle T_a^b \rangle$  evaluated for the extremal configuration is divergent as  $y \rightarrow 1$ . Indeed, for  $q = \sqrt{2}$  the components of the stress-energy tensor behave as  $(y-1)^{-3}$ . This is in a sharp contrast with the Reissner–Nordström case, in which the stress-energy tensor approaches

$$\langle T_a^b \rangle = \frac{1}{2880\pi^2 m^2 M^6} \left[ \frac{16}{21} - \left( \xi - \frac{1}{6} \right) \right] \text{diag}[1, 1, -1, -1] \quad (3.25)$$

as  $y \rightarrow 1$ . It should be noted however, that, except  $a = 0$ , the region in the vicinity of the degenerate horizon of the extremal geometry is beyond the applicability of the Schwinger–DeWitt approximation. On the other hand, however, one expects that in the opposite limit, *i.e.* for  $q \ll 1$ , the appropriate components of the stress-energy tensor are almost indistinguishable.

To analyze  $\langle T_a^b \rangle$  for intermediate values of  $q$  let us refer to the numerical calculations. The plots of the time, radial and angular components of the stress-energy tensor of the quantized massive scalar field as a function of the rescaled radial coordinate for  $q = i/10$  ( $i = 0, \dots, 13$ ) in the most interesting region are displayed in figures 1–3. These graphs are supplemented by figure 4, where the dependence of the horizon values of  $\langle T_t^t \rangle = \langle T_r^r \rangle$  and  $\langle T_\theta^\theta \rangle = \langle T_\phi^\phi \rangle$  on  $q$  is presented. Inspection of the figures and comparison with the analogous results obtained for the Reissner–Nordström geometry indicates that even for the intermediate values of  $q$  there are still qualitative similarities. Indeed, the time and angular components attain (positive) maximum at the event horizon, decrease with  $r$  and approach (negative) minimum. The magnitude of the maximum and the modulus of the minimum increase with increasing  $q$ , and, consequently, so does the slope of the curves.

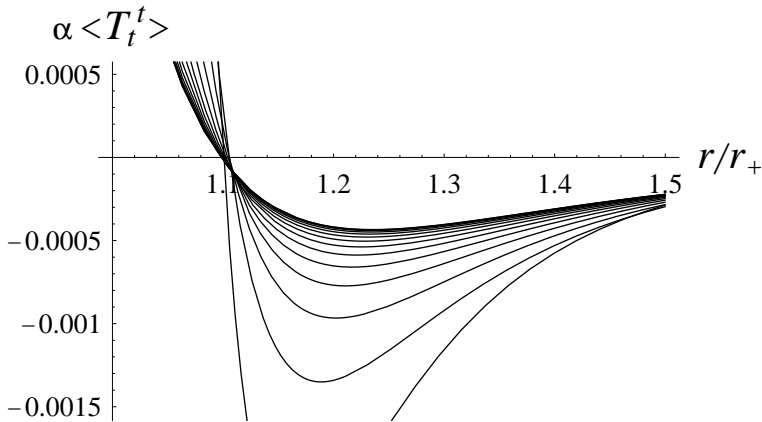


Fig. 1. This graph shows the radial dependence of the rescaled component  $\langle T_t^t \rangle$ , ( $\alpha = 192 \pi^2 M^6 m^2$ ) of the stress-energy tensor of the massive conformally coupled scalar field in the geometry of the dilatonic black hole with  $a = 1$  for  $q = i/10$ , ( $i = 0, \dots, 13$ ). In each case  $\langle T_t^t \rangle$  has its positive maximum at  $r_+$  and attains negative minimum away from the event horizon. The magnitude of the maximum and the modulus of the minimum increase with increasing  $q$ .

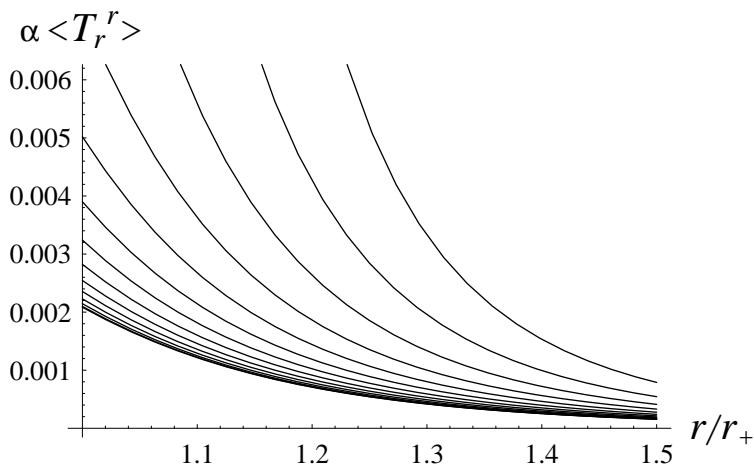


Fig. 2. This graph shows the radial dependence of the rescaled component  $\langle T_r^r \rangle$  ( $\alpha = 192\pi^2 M^6 m^2$ ) of the stress-energy tensor of the massive conformally coupled scalar field in the geometry of the dilatonic black hole with  $a = 1$  for  $q = i/10$ , ( $i = 0, \dots, 13$ ). Top to bottom the curves are plotted for decreasing values of  $q$ . In each case  $\langle T_r^r \rangle$  has its positive maximum at  $r_+$  and monotonically decreases with  $r$ .

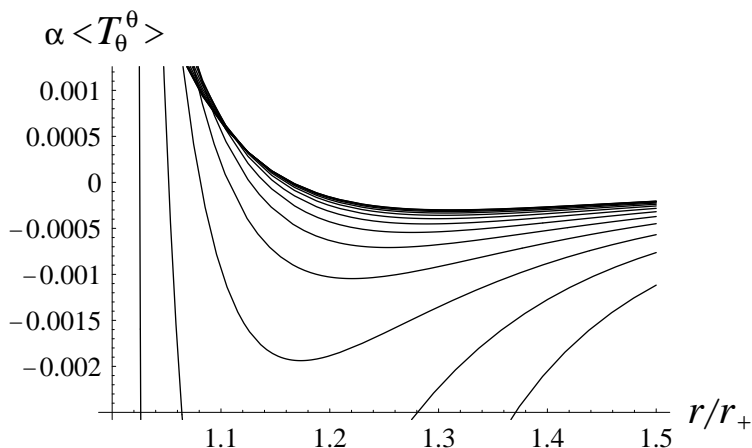


Fig. 3. This graph shows the radial dependence of the rescaled component  $\langle T_\theta^\theta \rangle$ , ( $\alpha = 192\pi^2 M^6 m^2$ ) of the stress-energy tensor of the massive conformally coupled scalar field in the geometry of the dilatonic black hole with  $a = 1$  for  $q = i/10$ , ( $i = 0, \dots, 13$ ). In each case  $\langle T_t^t \rangle$  has its positive maximum at  $r_+$  and attains negative minimum away from the event horizon. The magnitude of the maximum and the modulus of the minimum increase with increasing  $q$ ,

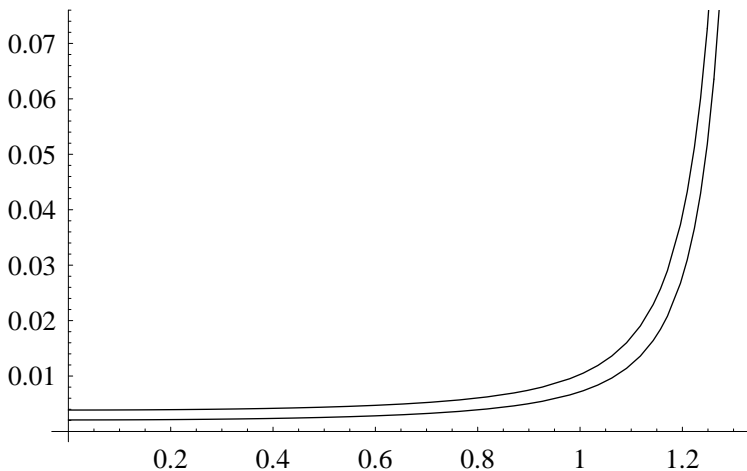


Fig. 4. This graph shows the horizon values of  $\langle T_\theta^\theta \rangle$  (upper curve) and  $\langle T_t^t \rangle$  (lower curve) as functions of  $q$ . On the event horizon  $\langle T_t^t \rangle = \langle T_r^r \rangle$  and because of the spherical symmetry one has  $\langle T_\theta^\theta \rangle = \langle T_\phi^\phi \rangle$ .

Before proceeding to physically interesting and important case  $\eta = -1/6$ , it is useful to study a role played by each  $T_a^{(i)b}$  separately. First, it could be easily shown that  $T_a^{(3)b}$  is negligible with respect to other terms, and, therefore, it does not contribute to the final result for reasonable values of the curvature coupling. The run of the resulting stress-energy tensor depends on a competition between remaining components. Indeed, inspection of figure 5 in which we exhibited  $T_t^{(i)t}$  as a function of the rescaled radial coordinate for fourteen exemplar values of  $q$  indicates that the term  $-T_a^{(1)b}$  produces the most prominent maximum at the event horizon for  $q \lesssim 0.9$  whereas for greater values of  $q$  this role is played by  $T_a^{(2)b}$ . General features of  $T_r^{(i)r}$  and  $T_\theta^{(i)\theta}$  are essentially the same.

Now the run of the stress-energy tensor as a function of  $q$  could be easily anticipated. The general structure remains, of course, of the form (3.16), but now the dominant contribution to the result is provided initially by the term  $\eta T_a^{(1)b}$  and subsequently with increasing  $q$  by the sum  $-1/6 T_a^{(1)b} + 1/36 T_a^{(2)b}$ . Moreover, since oscillatory-like behavior of  $T_a^{(3)b}$  does not play a significant role we have also qualitative similarities with the tensor evaluated for the conformal coupling.

Having computed  $\tilde{T}_a^{(i)b}$  and combining them with appropriate values of the coefficients  $\alpha_i$  for  $i = 1 \dots 10$ , after simplifications and rearrangement one has

$$\begin{aligned}
 f_0(y) &= \frac{1237}{210 y^3} - \frac{75}{14 y^2}, & f_1(y) &= -q^2 \left( \frac{377}{30 y^4} - \frac{703}{70 y^3} - \frac{9}{7 y^2} \right), \\
 f_2(y) &= q^4 \left( \frac{3637}{140 y^5} - \frac{5219}{140 y^4} + \frac{2259}{140 y^3} - \frac{99}{28 y^2} \right), \\
 f_3(y) &= -q^6 \left( \frac{84407}{3360 y^6} - \frac{11311}{280 y^5} + \frac{1177}{60 y^4} - \frac{99}{28 y^3} \right), \\
 f_4(y) &= q^8 \left( \frac{218839}{17920 y^7} - \frac{1097669}{53760 y^6} + \frac{11479}{1120 y^5} - \frac{3891}{2240 y^4} \right), \\
 f_5(y) &= -q^{10} \left( \frac{318457}{107520 y^8} - \frac{33919}{6720 y^7} + \frac{2639}{1024 y^6} - \frac{273}{640 y^5} \right), \\
 f_6(y) &= q^{12} \left( \frac{24685}{86016 y^9} - \frac{42557}{86016 y^8} + \frac{3139}{12288 y^7} - \frac{515}{12288 y^6} \right).
 \end{aligned} \tag{3.26}$$

The qualitative behavior of the stress-energy tensor of the minimally coupled scalar field is similar to the conformally coupled case, and, once again, for the intermediate values of  $q$  one has quantitative similarities with the Reissner–Nordström case. Moreover, from figure 5 one can easily deduce the general behavior of the stress-energy tensor for arbitrary coupling for  $q < 0.9$ .

Finally we remark, that the dilatonic black holes with  $a = 1$  or  $a = 0$  do not exhaust physically important solutions. For example for  $a = \sqrt{3}$  one has a four dimensional effective model reduced from the Kaluza–Klein theory in five dimensions. By (3.10) the approximate stress-energy tensor expressed in term of  $x$ ,  $x_+$  and  $x_-$  could be schematically written as

$$\langle T_a^b \rangle = \frac{p}{[x(x - x_-)]^{15/2}} \sum_{ijk} d_{ijk}^a [\eta] x^i x_+^j x_-^k, \tag{3.27}$$

where  $0 \leq i \leq 7$ ,  $0 \leq j \leq 3$  and  $0 \leq k \leq 6$  subjected to the condition  $i + j + k = 9$ . The qualitative behavior of the stress-energy tensor for both  $\eta = 0$  and  $\eta = -1/6$  is similar to  $\langle T_a^b \rangle$  constructed in the geometry of a dilatonic black hole with  $a = 1$  and its run for small  $q$  could be easily inferred from (3.15).

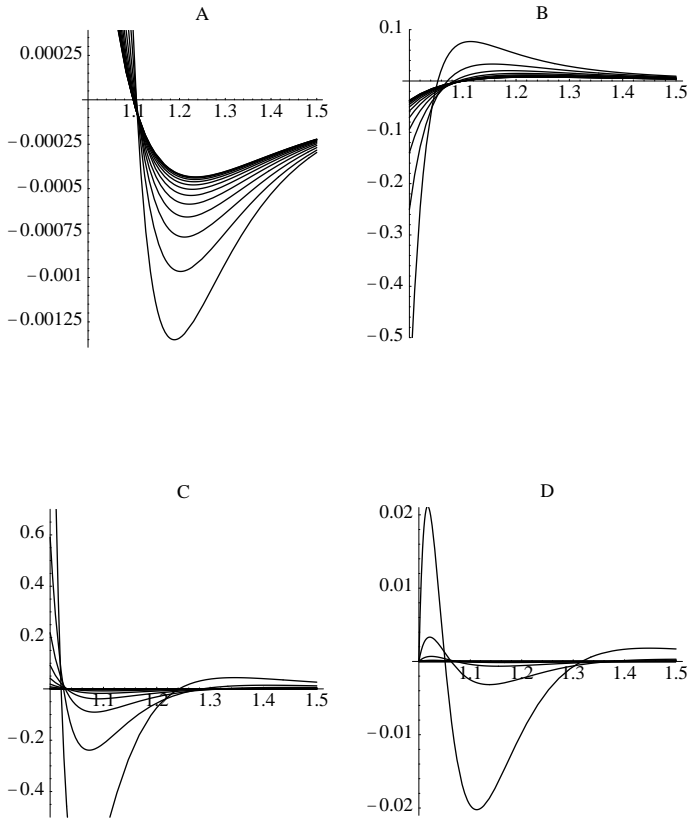


Fig. 5. This graph shows radial dependence of the rescaled  $T_t^{(0)t}$  (panel A),  $T_t^{(1)t}$  (panel B),  $T_t^{(2)t}$  (panel C) and  $T_t^{(3)t}$  (panel D) for  $q = i/10$  ( $i = 0, \dots, 13$ ). The scaling factor is  $192\pi^2 M^6 m^2$ . The magnitude of  $T_t^{(k)t}$  grows with increasing  $q$  for  $k = 0, 2$ , and  $3$ .

#### 4. Energy conditions

In the proofs of various theorems such as singularity theorems, positivity of mass or topological censorship it is assumed that the components of the stress-energy tensor of the matter fields do satisfy some restrictions usually addressed to as the energy conditions. And although the present status of the pointwise energy condition vary from disfavor to disbelief, to say the least, their detailed studies are worthwhile as their violation frequently leads to exotic yet physically interesting situations. It is well-known that the quantum fields violate the energy conditions, and, moreover, similar violations has been encountered even at the classical level. Hence, in spite of the fact that all available informations of the quantum field theory in curved

background are encoded in the components of the stress-energy tensor, one can get a better understanding of the physical nature of the quantized fields propagating in the spacetime of the dilatonic black hole analyzing the rate of possible violations of the energy conditions.

Here we briefly analyze various pointwise energy conditions but before proceeding further we shall examine the energy density itself. Since the components of the stress-energy tensor depend in general on the electric and dilatonic charges, the coupling constant and radial coordinate in rather complicated form we shall concentrate on the particular combinations of charges and couplings. It should be noted that the results for extremal and near-extremal dilatonic black hole should not be treated too seriously as geometries of such configurations are beyond the applicability of the Schwinger–DeWitt approximation. Therefore, in the following, we shall restrict ourselves to the solutions with  $0 \leq q \leq 1.3$  (although sometimes we quote the appropriate results for the extremal configurations as they provide useful bounds).

To simplify discussion let us introduce the energy density of the quantized fields,  $\rho$ , defined as

$$\rho = -\langle T_t^t \rangle, \quad (4.1)$$

and the three principal pressures,  $p_i$ , connected to the diagonal components of the stress-energy tensor as

$$p_1 = \tau = -\langle T_r^r \rangle \quad (4.2)$$

and

$$p_2 = p_3 = p = \langle T_\theta^\theta \rangle. \quad (4.3)$$

For  $a = 1$  and conformal coupling with curvature one has to consider two cases:  $0 \leq q < q_c$  and  $q_c \leq q < \sqrt{2}$ , where  $q_c = \sqrt{18 - \sqrt{286}} \approx 1.043$ . For  $q \leq q_c$  the energy density is negative in the narrow strip near the event horizon,  $1 \leq x < x_1$  and positive elsewhere, whereas for  $q > q_c$  the energy density is positive in the region  $x_1 \leq x \leq x_2$ . Numerically,  $x_1 = 1.098$  for  $q = 0$  and  $x_1 = 1.2479$  for  $q = \sqrt{2}$ ; in the extremality limit  $x_2 = 1.747$ . On the other hand for a minimal coupling, the energy density  $\rho$  function has only one real root,  $x_1 > 1$ , located slightly outside the event horizon and is positive for  $x \geq x_1$ .

#### 4.1. Null energy condition

It is said that the matter field satisfies the null energy conditions if for any null vector  $k^a$

$$T_{ab}k^ak^b \geq 0, \quad (4.4)$$

or, equivalently

$$\rho + p_i \geq 0, \quad (4.5)$$

for  $i = 1, 2, 3$ . In the spacetime at hand conditions (4.5) reduce to

$$\rho - \tau \geq 0 \quad (4.6)$$

and

$$\rho + p \geq 0. \quad (4.7)$$

Inspection of the exact results indicate that the first condition is satisfied for all distances, as

$$\rho - \tau \sim \frac{x-1}{(2x-q^2)x^9} W_6(x; q) \quad (4.8)$$

and the 6-th order polynomial  $W_6(x; q)$  has no real roots for  $x \geq 1$ . The second one is satisfied only in a finite region  $1 \leq x \leq x_3$ , where  $x_3(q)$  is a decreasing function of  $q$ , with  $x_3 = 9/5$  for  $q = 0$ . Therefore, the null energy condition is satisfied in a narrow strip in the vicinity of the event horizon.

Similarly, for the minimal coupling the question of whether or not the null energy condition is satisfied is in fact the question of non-negativity of  $\rho + p$  as the second constraint is always satisfied. A closer examination indicates that  $\rho + p$  is positive near the event horizon and negative elsewhere.

#### 4.2. Weak energy condition

The stress-energy tensor satisfies the weak energy condition if for any timelike vector  $X^a$

$$T_{ab} X^a X^b \geq 0 \quad (4.9)$$

or in terms of the energy density and principal pressures

$$\begin{aligned} \rho + p_i &\geq 0, \\ \rho &\geq 0, \end{aligned} \quad (4.10)$$

and, consequently, the weak energy condition is equivalent to the null energy condition supplemented by the constraint  $\rho > 0$  that has already been discussed. It follows then that for  $q > 1.01$  the weak energy condition is violated everywhere, whereas for  $0 < q < 1.01$  it is satisfied in a small region near the event horizon. On the other hand, for  $\xi = 0$ , the weak energy condition is satisfied only in a narrow strip located near the event horizon and is violated in its closest vicinity.

### 4.3. Strong energy condition

The strong energy condition is equivalent to the three constraints

$$\begin{aligned}\rho + p_i &\geq 0, \\ \rho + \sum_i p_i &\geq 0\end{aligned}\tag{4.11}$$

or, equivalently to (4.6) and (4.7), supplemented by

$$\rho - \tau + 2p \geq 0.\tag{4.12}$$

Numerical calculations carried out for  $\xi = 1/6$  indicate that for  $q \leq q_1 = 0.6345$  the constraint (4.12) is more restrictive than (4.7). On the other hand, for  $q \geq q_1$  the strong energy condition is equivalent to the null energy condition. It follows then that the strong energy condition is violated everywhere outside the narrow strip in the vicinity of the event horizon and the magnitude of this region is decreasing function of  $q$ . For the minimal coupling the qualitative behavior of the stress-energy tensor remains the same.

### 4.4. Dominant energy condition

The stress-energy tensor satisfies the dominant energy condition if the locally measured energy density is positive and the energy flux is timelike or null. In terms of the energy density and principal pressures one has  $\rho \geq 0$  and

$$-\rho \leq p_j \leq \rho.\tag{4.13}$$

Qualitative behavior of the energy density and the principal pressures for both considered couplings is similar: for small  $q$  and small as well as intermediate values of the radial coordinate there are regions where the energy density dominates the principal pressures, whereas for large  $r$  this energy condition is violated for any value of  $q$ . It is because the function  $\rho + p$  has only one real root, say  $x_a$ , and is negative for  $x > x_a$ .

From the above analysis one can draw a conclusion that even in the case of the weakest of the energy conditions, namely the null one, the region in which the energy condition is satisfied is small. It is therefore of principal interest to analyze the averaged energy conditions, and, what is even more important, the quantum inequalities.

## 5. Concluding remarks

In this paper we have constructed and examined the approximate renormalized stress-energy tensor of the massive scalar field in the spacetime of the static electrically charged dilatonic black hole with the special emphasis

put on the string inspired case  $a = 1$ . The method employed here is based on the observation that the lowest order of the expansion of the effective action in  $m^{-2}$  could be expressed in terms of the integrated coincidence limit of coefficient  $a_3(x, x')$ . Although the line element of the dilatonic black hole has a simple form, the analytical formulas describing the stress-energy tensor for a general  $a$  constructed within the Schwinger–DeWitt framework are extremely complicated and hence hard to utilize. Fortunately, for a concrete choice of  $a$  there are massive simplifications.

Expanding for  $q \ll 1$  the stress-energy tensor into a power series it is possible to analyze the influence of  $a$  on  $\langle T_a^b \rangle$ . For  $q = 0$  it reduces to the result derived by Frolov and Zel'nikov whereas for small values of  $q$  the stress-energy tensor resembles that evaluated in the Reissner–Nordström geometry. The discrepancies between the tensors grow with  $q$ . It should be stressed however that in the opposite limit the Schwinger–DeWitt technique is inapplicable.

The problem of the massless fields certainly deserves separate treatment, this however would require extensive numerical calculations as even for simplest case of the Schwarzschild geometry existing analytical approximations give, at best, only qualitative agreement with the exact results. At the moment we only know that the horizon value of the field fluctuation [32]

$$\langle \phi^2 \rangle = \frac{1}{48\pi^2 M^2 x_+^2} \left[ 1 - \frac{x_-}{(1+a^2)x_+} \right] \left( 1 - \frac{x_-}{x_+} \right)^{-\frac{2a^2}{1+a^2}}, \quad (5.1)$$

which is divergent in the extremality limit for  $a > 0$ . This suggests that the stress-energy tensor is also divergent at  $r_+$  of the extremal case. On the other hand, a first non-vanishing term of the approximation to the field fluctuation for a massive field is simply

$$\langle \phi^2 \rangle = \frac{1}{16\pi^2 m^2} [a_2] + \mathcal{O}(m^{-4}), \quad (5.2)$$

and it could be easily shown that

$$\langle \phi^2 \rangle = \frac{f(a, r_+, r_-)}{720\pi^2 m^2 M^4 x_+^6} (1+a^2)^{-2} \left( 1 - \frac{x_-}{x_+} \right)^{-\frac{4a^2}{1+a^2}} + \mathcal{O}(m^{-4}), \quad (5.3)$$

where

$$f(a, r_+, r_-) = [4 + 3a^2(1 - 5\xi)] x_-^2 - 6(1 + a^2) x_+ x_- + 3(1 + a^2)^2 x_+^2. \quad (5.4)$$

As the realistic calculations of the stress-energy tensor of the quantized massless fields are expected to be extremely complicated, it is natural to

analyze some simpler models first. Such calculations in a spacetime of 2D dilatonic black holes with the emphasis put on the extremal configurations have been carried out in Ref. [33]. It should be noted, however, that the solution of the Einstein–Maxwell-dilaton system when specialized to two dimensions reduces to 2D Schwarzschild line element, and, unfortunately, all interesting physics connected with the angular term is lost. On the other hand the string metric solution analyzed at length in [33] is not considered here.

Finally, we make some comments regarding applications and generalizations of the results presented in this paper. The question of the massless field has been addressed above. A careful analysis carried out for  $a = 0$  in Ref. [41] shows that at least up to  $\mathcal{O}(m^{-4})$  the adapted method approximates well the field fluctuation of the massive field in the thermal state of temperature  $T_H$ . It would be interesting to extend this analysis for any value of  $a$ .

It should be stressed that because of special character of the line element (2.2) the approximation derived in Refs [16] and [17] is the only one that allows construction of the renormalized stress-energy tensor in the geometry of the dilaton black hole. Moreover, it could be easily modified to incorporate quantized massive spinor and vector fields. We also remark that the derived stress-energy tensors may be employed as a source term of the semiclassical Einstein field equations. Indeed, preliminary calculations indicate that it is possible to construct the solution to the linearized semiclassical Einstein–Maxwell-dilaton equations. We hope that presented results will be of use in subsequent applications. We intend to return to this group of problems elsewhere.

## Appendix

### *Coincidence limits of the coefficients $a_2(x, x')$ and $a_3(x, x')$*

In this appendix we list coincidence limits of the coefficients  $a_2(x, x')$  and  $a_3(x, x')$  for the scalar field equation (1.1). With the normalization employed in this paper the coefficient  $[a_2]$  reads

$$[a_2] = -\frac{1}{6} \left( \xi - \frac{1}{5} \right) \square R + \frac{1}{2} \left( \xi - \frac{1}{6} \right)^2 R^2 + \frac{1}{180} \left( R_{abcd} R^{abcd} - R_{ab} R^{ab} \right), \quad (\text{A.1})$$

whereas  $[a_3]$  could be written as

$$[a_3] = \frac{b_3}{7!} + \frac{c_3}{360}, \quad (\text{A.2})$$

where

$$\begin{aligned}
 b_3 = & \frac{35}{9}R^3 + 17R_{;p}R^{;p} - R_{qa;p}R^{qa;q} - 4R_{qa;p}R^{pa;q} \\
 & + 9R_{qabc;p}R^{qabc;p} + 2R\Box R + 18\Box^2 R - 8R_{pq}\Box R^{pq} - \frac{14}{3}RR_{pq}R^{pq} \\
 & + 24R_{pq;a}R^{pa} - \frac{208}{9}R_{pq}R^{qa}R_a{}^p + 12\Box R_{pqab}R^{pqab} + \frac{64}{3}R_{pq}R_{ab}R^{pqab} \\
 & - \frac{16}{3}R_{pq}R^p{}_{abc}R^{qabc} + \frac{80}{9}R_{pqab}R_c{}^p{}_d{}^a R^{qcbd} + \frac{44}{9}R_{pqab}R_{cd}{}^{pq}R^{abcd} \quad (A.3)
 \end{aligned}$$

and

$$\begin{aligned}
 c_3 = & -(5\xi - 30\xi^2 + 60\xi^3)R^3 - (12\xi - 30\xi^2)R_{;p}R^{;p} - (22\xi - 60\xi^2)R\Box R \\
 & - 6\xi\Box^2 R - 4\xi R_{pq}R^{pq} + 2\xi RR_{pq}R^{pq} - 2\xi RR_{pqab}R^{pqab}. \quad (A.4)
 \end{aligned}$$

*$\langle T_a^b \rangle$  of the massive scalar fields in the spacetime of the  
Reissner–Nordström black hole*

Inserting curvature tensor and its covariant derivatives into the general formulas obtained from functional differentiation of the effective action (3.1) with respect to the metric tensor one obtains the approximate stress-energy tensor of massive fields. Since the curvature scalar of the Reissner–Nordström geometry is zero, one expects considerable simplifications. Indeed, it could be easily shown that the tensors  $\tilde{T}_a^{(1)b}$  and  $\tilde{T}_a^{(3)b}$  do not contribute to the final result. The stress-energy tensor of the massive scalar field with arbitrary coupling with curvature in the Reissner–Nordström geometry has the form (3.8), where

$$\begin{aligned}
 T_t^{(0)t} = & \frac{313}{7}x^3 - \frac{285}{14}x^4 + q^2 \left( \frac{-769}{14}x^2 - \frac{192}{7}x^3 + \frac{135}{7}x^4 \right) \\
 & + q^4 \left( \frac{514}{7}x - \frac{101}{21}x^2 \right) - \frac{208}{7}q^6, \quad (A.5)
 \end{aligned}$$

$$\begin{aligned}
 T_r^{((0)r)} = & -11x^3 + \frac{15}{2}x^4 + q^2 \left( \frac{709}{14}x^2 - \frac{248}{7}x^3 + \frac{27}{7}x^4 \right) \\
 & + q^4 \left( -46x + \frac{421}{21}x^2 \right) + \frac{74}{7}q^6, \quad (A.6)
 \end{aligned}$$

$$\begin{aligned}
 T_\theta^{(0)\theta} = & \frac{367}{7}x^3 - \frac{45}{2}x^4 + q^2 \left( \frac{-3303}{14}x^2 + \frac{814}{7}x^3 - \frac{81}{7}x^4 \right) \\
 & + q^4 \left( \frac{1726}{7}x - \frac{1522}{21}x^2 \right) - 73q^6, \quad (A.7)
 \end{aligned}$$

$$T_t^{(1)t} = -792 x^3 + 360 x^4 + q^2 (2604 x^2 - 1008 x^3) + q^4 (-2712 x + 728 x^2) + 819 q^6, \quad (\text{A.8})$$

$$T_r^{(1)r} = 216 x^3 - 144 x^4 + q^2 (-588 x^2 + 336 x^3) + q^4 (504 x - 208 x^2) - 117 q^6 \quad (\text{A.9})$$

and

$$T_\theta^{(1)\theta} = -1008 x^3 + 432 x^4 + q^2 (3276 x^2 - 1176 x^3) + q^4 (-3408 x + 832 x^2) + 1053 q^6. \quad (\text{A.10})$$

*Power expansion of the stress-energy tensor for  $q \ll 1$*

Repeating the calculations for the line element (2.2)–(2.3) one obtains components of the stress-energy tensor in the geometry of a general dilatonic black hole. Assuming  $q \ll 1$  and expanding the result into a power series, after the necessary simplifications (3.15), where the coefficients  $t_a^{(i)b}$  are given by

$$t_t^{(1)t} = \frac{939}{35} - \frac{76 x}{7} + \eta \left( 192 x - \frac{2376}{5} \right), \quad (\text{A.11})$$

$$t_r^{(1)r} = 4x - \frac{33}{5} + \eta \left( \frac{648}{5} - \frac{384 x}{5} \right), \quad (\text{A.12})$$

$$t_\theta^{(1)\theta} = \frac{1101}{35} - 12 x - \eta \left( \frac{3024}{5} - \frac{1152 x}{5} \right), \quad (\text{A.13})$$

$$\begin{aligned} t_t^{(2)t} = & \frac{1207}{140} - \frac{4359 a^2}{140} - \frac{9773}{210 x} + \frac{939 a^2}{14 x} + \frac{181 x}{105} + \frac{19 a^2 x}{7} - \frac{x^2}{14} \\ & + \eta \left( \frac{2754 a^2}{5} - \frac{1594}{15} + \frac{888}{x} - \frac{1188 a^2}{x} - \frac{436 x}{5} - 48 a^2 x + 12 x^2 \right) \\ & + \eta^2 \left( -6076 + \frac{6000}{x} + 1908 x - 180 x^2 \right), \end{aligned} \quad (\text{A.14})$$

$$\begin{aligned} t_r^{(2)r} = & -\frac{12091}{1260} + \frac{213 a^2}{20} + \frac{3793}{210 x} - \frac{33 a^2}{2 x} + \frac{83 x}{315} - a^2 x + \frac{11 x^2}{70} \\ & + \eta \left( 58 - \frac{1026 a^2}{5} - \frac{1032}{5 x} + \frac{324 a^2}{x} + \frac{388 x}{15} + \frac{96 a^2 x}{5} - \frac{24 x^2}{5} \right) \\ & + \eta^2 \left( 1556 - \frac{1200}{x} - 612 x + 72 x^2 \right) \end{aligned} \quad (\text{A.15})$$

$$\begin{aligned}
t_{\theta}^{(2)\theta} &= \frac{6841}{252} - \frac{4881 a^2}{140} - \frac{18139}{210 x} + \frac{1101 a^2}{14 x} + \frac{227 x}{315} + 3 a^2 x - \frac{33 x^2}{70} \\
&+ \eta \left( \frac{3348 a^2}{5} + \frac{5572}{5 x} - \frac{1512 a^2}{x} - \frac{1628 x}{15} - \frac{288 a^2 x}{5} + \frac{72 x^2}{5} - \frac{296}{3} \right) \\
&+ \eta^2 \left( -7232 + \frac{7200}{x} + 2268 x - 216 x^2 \right),
\end{aligned}
\tag{A.16}$$

$$\begin{aligned}
t_t^{(3)t} &= \frac{4847}{840} - \frac{4138 a^2}{315} + \frac{4359 a^4}{280} + \frac{20149}{420 x^2} - \frac{24971 a^2}{210 x^2} + \frac{3443 a^4}{28 x^2} \\
&- \frac{9059}{420 x} + \frac{6026 a^2}{105 x} - \frac{297 a^4}{4 x} - \frac{79 x}{210} + \frac{152 a^2 x}{105} - \frac{19 a^4 x}{14} - \frac{x^2}{28} + \frac{a^2 x^2}{28} \\
&+ \eta \left( \frac{5642 a^2}{5 x^2} - \frac{1294}{15} - \frac{662 a^2}{5} - \frac{1377 a^4}{5} - \frac{4346}{5 x^2} - \frac{2178 a^4}{x^2} + \frac{1936}{5 x} \right. \\
&- \frac{278 a^2}{15 x} + \frac{1314 a^4}{x} - \frac{78 x}{5} + \frac{198 a^2 x}{5} + 24 a^4 x + 6 x^2 - 6 a^2 x^2 \left. \right) \\
&+ \eta^2 \left( 7634 a^2 - 658 - \frac{2232}{x^2} + \frac{21984 a^2}{x^2} + \frac{696}{x} - \frac{21596 a^2}{x} + 534 x \right. \\
&- 1254 a^2 x - 90 x^2 + 90 a^2 x^2 \left. \right),
\end{aligned}
\tag{A.17}$$

$$\begin{aligned}
t_r^{(3)r} &= -\frac{1783}{840} + \frac{187 a^2}{70} - \frac{213 a^4}{40} - \frac{5009}{420 x^2} + \frac{5111 a^2}{210 x^2} - \frac{121 a^4}{4 x^2} \\
&+ \frac{401}{60 x} - \frac{4352 a^2}{315 x} + \frac{93 a^4}{4 x} + \frac{109 x}{630} - \frac{2 a^2 x}{45} + \frac{a^4 x}{2} + \frac{11 x^2}{140} - \frac{11 a^2 x^2}{140} \\
&+ \eta \left( \frac{86}{3} + \frac{188 a^2}{5} + \frac{513 a^4}{5} + \frac{158}{x^2} - \frac{250 a^2}{x^2} + \frac{594 a^4}{x^2} - \frac{96}{x} + \frac{118 a^2}{5 x} \right. \\
&- \frac{450 a^4}{x} + \frac{18 x}{5} - \frac{66 a^2 x}{5} - \frac{48 a^4 x}{5} - \frac{12 x^2}{5} + \frac{12 a^2 x^2}{5} \left. \right) \\
&+ \eta^2 \left( 130 - 2442 a^2 + \frac{288}{x^2} - \frac{4656 a^2}{x^2} - \frac{60}{x} + \frac{5764 a^2}{x} \right. \\
&- 166 x + 454 a^2 x + 36 x^2 - 36 a^2 x^2 \left. \right),
\end{aligned}
\tag{A.18}$$

$$\begin{aligned}
 t_{\theta}^{(3)\theta} = & \frac{2411}{360} - \frac{7267 a^2}{1260} + \frac{4881 a^4}{280} + \frac{29963}{420 x^2} - \frac{8857 a^2}{70 x^2} + \frac{4037 a^4}{28 x^2} - \frac{13 x}{315} \\
 & - \frac{11617}{420 x} + \frac{2792 a^2}{63 x} - \frac{2361 a^4}{28 x} - \frac{31 a^2 x}{90} - \frac{3 a^4 x}{2} - \frac{33 x^2}{140} + \frac{33 a^2 x^2}{140} \\
 & + \eta \left( \frac{1378 a^2}{x^2} - \frac{1252}{15} - \frac{926 a^2}{5} - \frac{1674 a^4}{5} - \frac{5214}{5 x^2} - \frac{2772 a^4}{x^2} + \frac{2052}{5 x} \right. \\
 & + \frac{976 a^2}{15 x} + \frac{1620 a^4}{x} - \frac{108 x}{5} + \frac{252 a^2 x}{5} + \frac{144 a^4 x}{5} + \frac{36 x^2}{5} - \left. \frac{36 a^2 x^2}{5} \right) \\
 & + \eta^2 \left( 9182 a^2 - 870 - \frac{2970}{x^2} + \frac{26640 a^2}{x^2} + \frac{1098}{x} - \frac{26008 a^2}{x} \right. \\
 & \left. + 644 x - 1508 a^2 x - 108 x^2 + 108 a^2 x^2 \right). \tag{A.19}
 \end{aligned}$$

The terms containing  $\eta^3$  appear starting from  $q^8$ .

## REFERENCES

- [1] N.B. Birrell, P.C.W. Davies, *Quantum Fields in Curved Space*, Cambridge University Press, Cambridge 1982.
- [2] J.S. Schwinger, *Phys. Rev.* **82**, 664 (1951).
- [3] B.S. DeWitt, *Dynamical Theory of Groups and Fields*, Gordon Breach, New York 1965.
- [4] B.S. DeWitt, *Phys. Rep.* **19C**, 297 (1975).
- [5] V.P. Frolov, A.I. Zel'nikov, *Phys. Lett.* **B115**, 372 (1982).
- [6] V.P. Frolov, A.I. Zel'nikov, *Phys. Lett.* **B123**, 197 (1983).
- [7] V.P. Frolov, A.I. Zel'nikov, *Phys. Rev.* **D29**, 1057 (1984).
- [8] G.W. Gibbons, *General Relativity: An Einstein Centenary Survey*, ed. S.W. Hawking and W. Israel, Cambridge University Press, Cambridge 1979.
- [9] T. Sakai, *Tohoku Math. J.* **23**, 589 (1971).
- [10] P.B. Gilkey, *Differential Geometry* **10**, 601 (1975).
- [11] P.B. Gilkey, *Trans. Am. Math. Soc.* **225**, 341 (1977).
- [12] I.G. Avramidi, Ph. D. Thesis (1986).
- [13] I.G. Avramidi, *Theor. Math. Phys.* **79**, 494 (1989).
- [14] I.G. Avramidi, *Nucl. Phys.* **B355**, 712 (1991).
- [15] P. Amsterdamski, A.L. Berkin, D.J. O'Connor, *Class. Quantum Grav.* **6**, 1981 (1989).
- [16] J. Matyjasek, *Phys. Rev.* **D61**, 124019 (2000).

- [17] J. Matyjasek, *Phys. Rev.* **D63**, 084004 (2001).
- [18] P.R. Anderson, W.A. Hiscock, D.A. Samuel, *Phys. Rev.* **D51**, 4337 (1995).
- [19] A.A. Popov, *Phys. Rev.* **D67**, 044021 (2003).
- [20] B.E. Taylor, W.A. Hiscock, P.R. Anderson, *Phys. Rev.* **D61**, 084021 (2000).
- [21] W.A. Hiscock, S.L. Larson, P.R. Anderson, *Phys. Rev.* **D56**, 3571 (1997).
- [22] B.E. Taylor, W.A. Hiscock, P.R. Anderson, *Phys. Rev.* **D55**, 6116 (1997).
- [23] J. Matyjasek, O.B. Zaslavskii, *Phys. Rev.* **D64**, 104018 (2001).
- [24] W. Berej, J. Matyjasek, *Phys. Rev.* **D66**, 024022 (2002).
- [25] L.A. Kofman, V. Sahni, *Phys. Lett.* **B127**, 197 (1983).
- [26] A.A. Starobinsky, L.A. Kofman, V. Sahni, *Zh. Eksp. Teor. Fiz.* **85**, 1876 (1983).
- [27] P.B. Groves, P.R. Anderson, E.D. Carlson, *Phys. Rev.* **D66**, 124017 (2002).
- [28] G.W. Gibbons, K. Maeda, *Nucl. Phys.* **B298**, 741 (1988).
- [29] D. Garfinkle, G.T. Horowitz, A. Strominger, *Phys. Rev.* **D43**, 3140 (1991).
- [30] J. Koga, K. Maeda, *Phys. Rev.* **D52**, 7066 (1995).
- [31] S. Alexeyev, A. Barrau, O. Boudoul, O. Khovanskaya, M. Sazhin, *Class. Quantum Grav.* **19**, 4431 (2002).
- [32] K. Shiraishi, *Mod. Phys. Lett.* **A7**, 3569 (1992).
- [33] D.J. Loran, W.A. Hiscock, *Phys. Rev.* **D55**, 3893 (1997).
- [34] R.C. Myers, *Nucl. Phys.* **B289**, 701 (1987).
- [35] C.G. Callan, R.C. Myers, M.J. Perry, *Nucl. Phys.* **B311**, 373 (1989).
- [36] V.P. Frolov, I.D. Novikov, *Physics of Black Holes*, Kluwer, New York 1999.
- [37] V.P. Frolov, Proceedings of the Lebedev Institute of the Academy of Science of USSR, 169.
- [38] S. W. Hawking, G.F.R. Ellis, *The Large Scale Structure of Space-Time*, Cambridge University Press, Cambridge 1973.
- [39] M. Visser, *Lorentzian Wormholes from Einstein to Hawking*, American Institute of Physics, New York 1995.
- [40] C. Barcelo, M. Visser, *Int. J. Mod. Phys.* **D11**, 1552 (2002).
- [41] H. Koyama, Y. Nambu, A. Tomimatsu, *Mod. Phys. Lett.* **15**, 815 (2000).